Marine Research
of the National Academy of Marine Research
ISSN: 2709-6629 (Vol.1 Iss.1)
GPN: 2011200033

DOI: http://dx.doi.org/10.29677/MR.202112_1(1).0001
2021, 1(1), 1-23

Characteristics of Sand Waves of the Changyun Sand Ridge and Taiwan Shoal in the Taiwan Strait

Liwen Chen [1*] Yi-Wei Lu [2] Wei-Chung Han [3] Sheng-Chung Lo [2]

[1] *National Academy of Marine Research, Ocean Affairs Council, Taiwan*
[2] *Green Energy and Environment Research Laboratories, Industrial Technology Research Institute, Taiwan*
[3] *Exploration and Development Research Institute, CPC Corporation, Taiwan*

ABSTRACT

Seabed topography reveals fundamental information of the earth system at multiple scales. Geomorphologic studies provide insights into the interaction between the hydrosphere and solid earth. We reviewed previous studies of the dynamic seabed environment in the Taiwan Strait and classified the sand waves of the Changyun Sand Ridge and Taiwan Shoal by compiling and analyzing the crest-line distribution and sand wave geometries. We identified five types of sand waves coexisting in the western Changyun Ridge, including long bed trochoidal (LT-type), symmetrical (S-type), trochoidal (T-type), sinusoidal (Sin-type) sand waves, and mega-ripples (Mr-type). Their heights (amplitudes) and wavelengths range from 4.5 to 37 m and 244 to 2,115 m, respectively. In Taiwan Shoal, trochoidal sand waves almost cover the entire area, while the sinusoidal and bimodal sand waves spread in the middle and western portions; the wave heights and wavelengths range from 0.3 to 10 meters and 5 to 1,700 meters, respectively. However, further time-dependent bathymetric and oceanographic investigations are required to simulate the long-term behavior of potential bedform variation along with extreme events. Monitoring the migration of sand waves will also contribute to understanding seabed stability and thus offshore engineering designs in the Taiwan Strait.

Keywords: seabed topography, geomorphology, Taiwan Strait, sand waves.

* Corresponding author, E mail: liwen@namr.gov.tw

Received 10 September 2021, Accepted 4 October 2021.

1 INTRODUCTION

Seafloor sand waves present typical transverse bedforms and are commonly found in tidal environments from estuaries to continental shelves (Allen, 1980). Sand waves are rhythmic bedforms with wavelengths between 100 and 1,000 meters and amplitudes greater than 1 meter (Ashley, 1990). Most seabed dynamics in offshore areas of sandy seafloor relate to the migration of sand waves (Van Dijk and Kleinhans, 2005). Sand waves are usually formed by erosion, sediment transportation, and deposition processes driven by the bottom tidal current and may occur in series or reform after disappearing. The development of sand waves indicates sediment movement, while the form drag produced by sand waves reduces bedload transport capability (Dyer and Soulsby, 1988). Thus, the conditions of local topography, sediment supply, currents, sea-level fluctuations, and climate changes may all affect the formation, distribution, and evolution of sand waves. Previous studies suggest that the size and shape of sand waves are controlled by current velocity, sediment particle size, and water depth (Rubin and McCulloch, 1980).

It is generally believed that sand waves generated by tidal currents migrate downstream (Németh et al., 2002); nonetheless, some simple mechanisms exist that cause the upstream-migrating sand waves in the opposite direction of the residual steady current (Besio et al., 2004). Sand wave migration is usually expressed as horizontal displacement over time, achieved by comparing repeated surveys in both plane (crest) and cross-sectional (profile) shapes (e.g., Van Dijk and Kleinhans, 2005; Barnard et al., 2011). Games and Gordon, 2015 present two case studies showing mass transport is potentially much more significant than expected, including its influence in the engineering designs of offshore wind turbines and power cables (Figure 1).

The science of morphodynamics involves bathymetry to fluid dynamic processes and their interactions (Wright and Thom, 1977). The formation and migration of seabed sediments are closely related to tidal currents, with sand ridges forming as rhythmic series, while sand waves are formed perpendicular to the current direction (Amos and King, 1984). As sand waves are dynamic, with the ability to migrate tens of meters or more per year, they pose potential hazards to engineered offshore and coastal structures, such as navigation channels, pipelines, and wind farms (Dorst et al., 2011). Therefore, a literature review and geomorphologic analysis were carried out in this study to better understand the nature and distribution of sand waves in the Taiwan Strait, where offshore wind energy has become a flourishing industry.

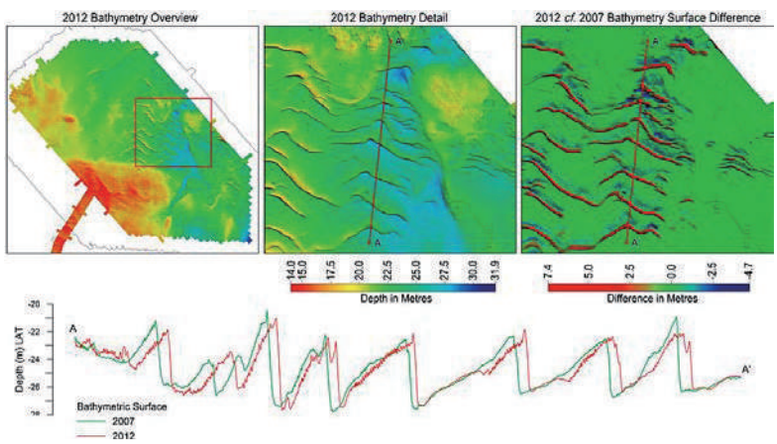

Figure 1. The sand wave observation in the North Sea suggests that the migration rate of large sand waves can be much higher than thought, with prominent features migrating up to 155 m in 5 years. (Games and Gordon, 2015)

Marine Research of the National Academy of Marine Research
DOI: 10.29677/MR.202112_1(1).0001

2 HYDRODYNAMICS AND SEABED ENVIRONMENT OF TAIWAN STRAIT

The submarine detritus sediments on the continental shelf constantly moves and accumulates, mainly dominated by the action of waves, tides, currents, and other hydrodynamic effects, shaping a variety of bedforms (Yincan et al., 2017). These hydrodynamic forces have various characteristics with significant differences in the direction, nature, size, and action mode, and the shaped bedforms. Therefore, the most important background study on marine sand waves considers the ocean's dynamic environment in the Taiwan Strait.

The Taiwan Strait connects the East China Sea (ECS) and South China Sea (SCS), playing an essential role in water and heat exchange between these two marginal seas. The Taiwan Strait is under the influence of the East Asia Monsoon (EAM), and this northeastern wind in winter can be extreme. In addition, an average of 3-5 typhoons (tropical storms) passes through the Taiwan region every year. Though the seafloor of the Taiwan Strait is shallow and relatively flat, it still presents series of complex topographic features, including the shallow Taiwan Shoal in its southwestern end and the steep-sided Penghu Channel lying between the Penghu Islands and Taiwan island in the southeastern part of the strait (Figure 2).

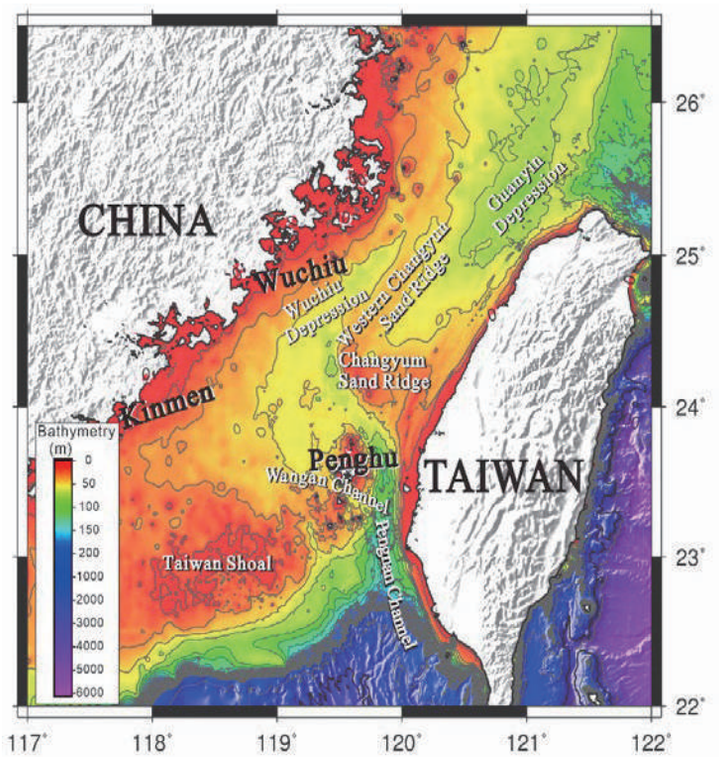

Figure 2. Seafloor morphological features in the Taiwan Strait. (names after Liu et al., 1998)

The unique geographic location, climate, and seafloor topography of the Taiwan Strait have influenced the physical processes of current-wave interaction in different scales of space and time, leading to various interesting ocean phenomena in this region. The transport of currents in the Taiwan Strait reveals stronger seasonal signals in summer than in winter (Jan et al., 2006; Wu and Hsin, 2005). The distribution of the flow rate at 30 m of depth (Figures 3a and b) and 15 m of depth (Figures 3c and d) derived from the shipboard Acoustic Doppler Current Profilers (ADCP) and the drifter tracks (Figure 3) have more similar patterns in summer than in

Marine Research of the National Academy of Marine Research
DOI: 10.29677/MR.202112_1(1).0001

winter, especially in the Taiwan Strait (Liang et al., 2003; Chang et al., 2008). Moreover, the tides in the Taiwan Strait are predominantly semidiurnal. Jan et al. (2004) demonstrated that the wave reflection of the southward propagating tidal wave by the deep channel in the southern strait caused a complex wave propagation pattern, resulting in wave resonance around the center of the strait. The sea waves are well developed in the Taiwan Strait area due to a combination of strong and stable northeast monsoons, and seasonal variation in sea waves are prominently affected by the monsoon (Wang, 2004). Based on sporadic tidal observations, semidiurnal waves are the dominant waves in the Taiwan Strait that reveal the coexisting propagating and standing wave systems. This standing wave system is consistent with the small energy dissipation in the central Taiwan Strait and significant energy dissipation in the south, where the shallow water effect also contributes to the local dissipation (Yu et al., 2017).

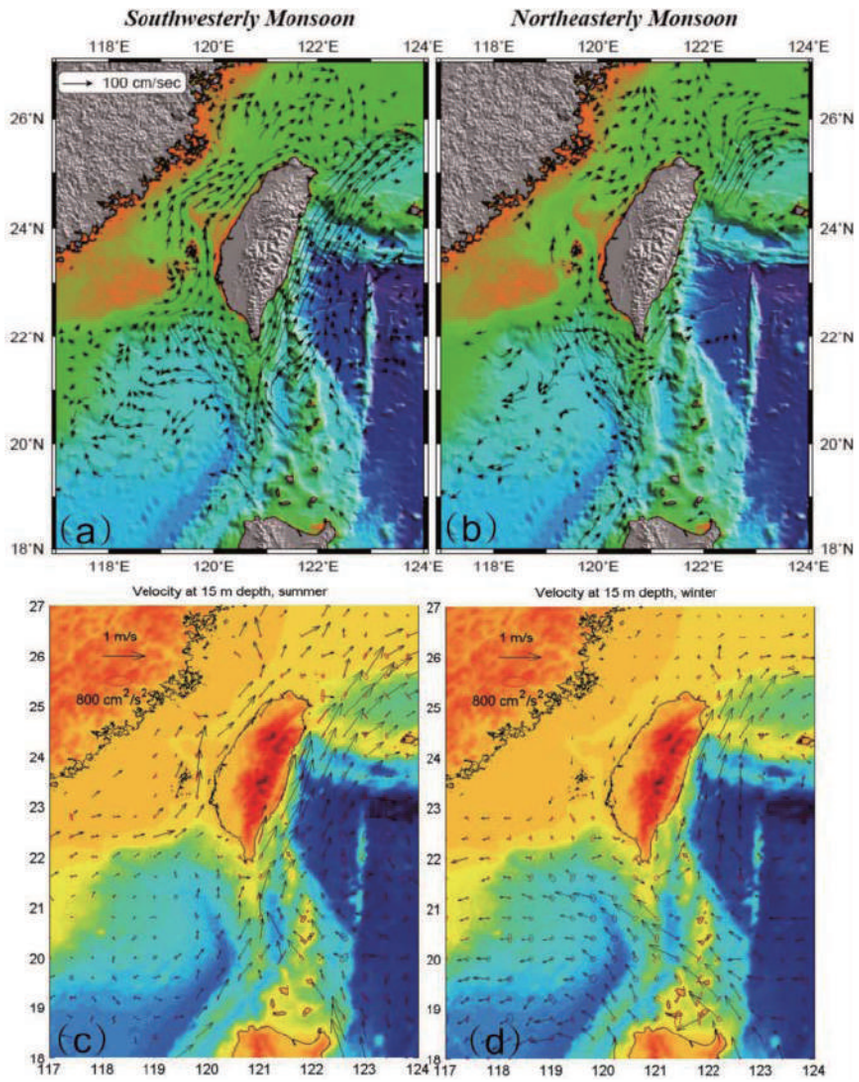

Figure 3. The current velocity at 30 m (a & b) and 15 m depth (c & d) derived from the Sb-ADCP and the drifter tracks, respectively. (after Chang et al., 2008)

Marine Research of the National Academy of Marine Research
DOI: 10.29677/MR.202112_1(1).0001

Hydrodynamics and sedimentation processes together drive the active fine-grain sediment transportation and result in the little seabed mud patches in the Taiwan Strait (Figure 4) (Kao et al., 2008). The apparent sediment accumulation rates derived from ^{210}Pb and ^{137}Cs profiles vary from 0.1 to 4.2 cm/yr (Figure 5). Spatial-temporal variations of the ^{7}Be activity of surface sediments indicate the episodic deposition of flood layers and their mobility from river estuaries toward the north (Huh et al., 2011).

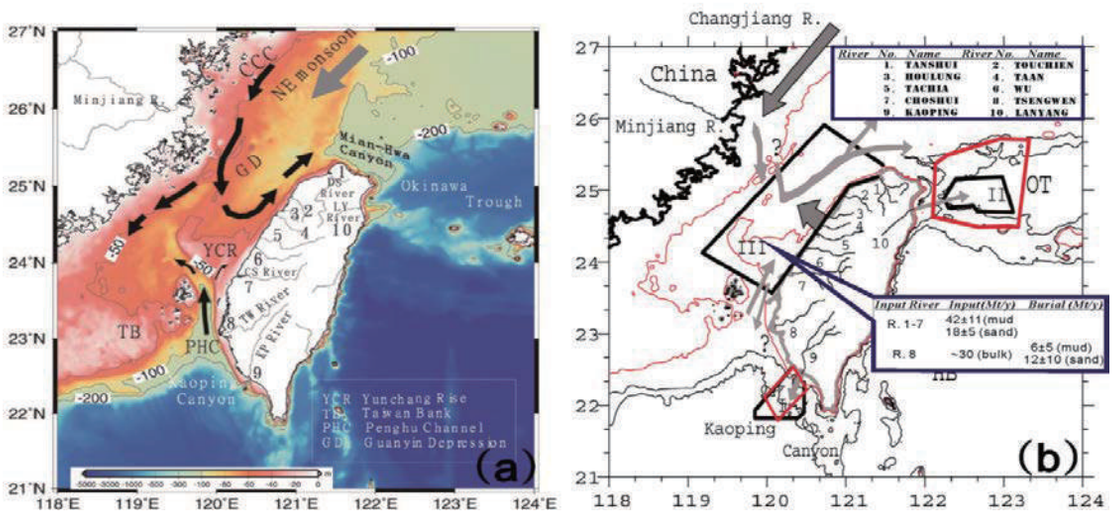

Figure 4. (a) Winter circulation patterns (black arrows) and the direction of the northeastern monsoon (gray arrows) in the Taiwan Strait. (Jan et al., 2004) (b) Sum of the potential sources (input rivers) and input-output fluxes (Mt/y) in the Taiwan Strait (III). The part of the fluxes from Minjiang and Changjian of China is unknown. (after Kao et al., 2008)

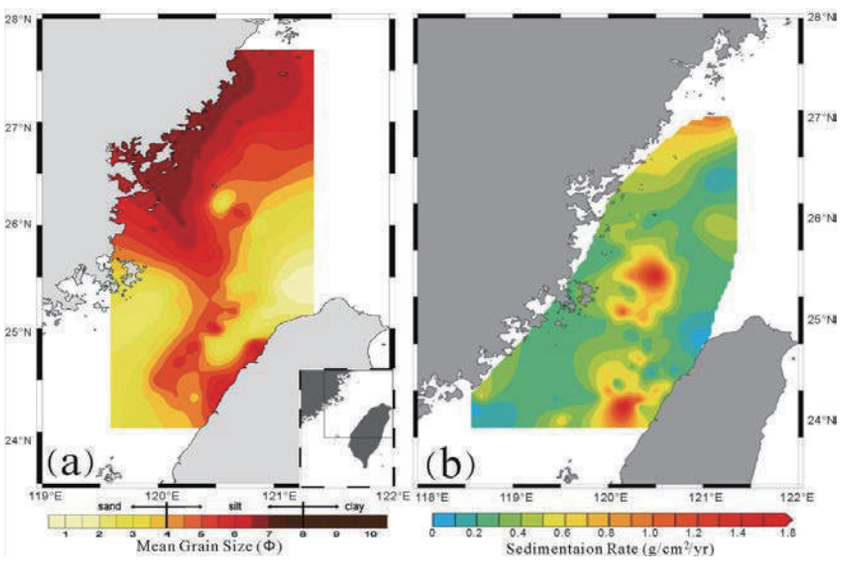

Figure 5. Distribution maps of (a) mean grain size of the surface sediments, (b) sedimentation rate derived from 210Pb inventory ratio in the Taiwan Strait. (after Huh et al., 2011)

DOI: 10.29677/MR.202112_1(1).0001

Located in the central Taiwan Strait, the Changyun Sand Ridge acts as the predominant topographic feature (Figure 2). Widespread asymmetrical sand waves with variable orientations in the Taiwan Strait (Figure 6a) suggest the active transportation of seafloor sediments driven by the bottom currents (Boggs, 1974). The chirp sonar profiles show a subaqueous delta prograde southwestward off the Choshui River mouth (Figure 6b). The clinoform is dominated by distinct sand waves about 2–5 m high (Liu et al., 2008). Liao and Yu (2005) describes the large to huge sand waves sequentially developed on the western Changyun Ridge, revealing their formations are likely controlled by the northward-flowing tidal currents (Figure 6c). According to Guan (2017), the sand wave migration rate in the Taiwan Strait can be as high as 2 m/day toward the northeast. The side-scan sonar images show at least three different sand wave shapes in the western shore of the Taiwan Strait (Figure 7), including unimodal shape, curved shape, and outcrop bedrock sand waves (Cai et al., 1992).

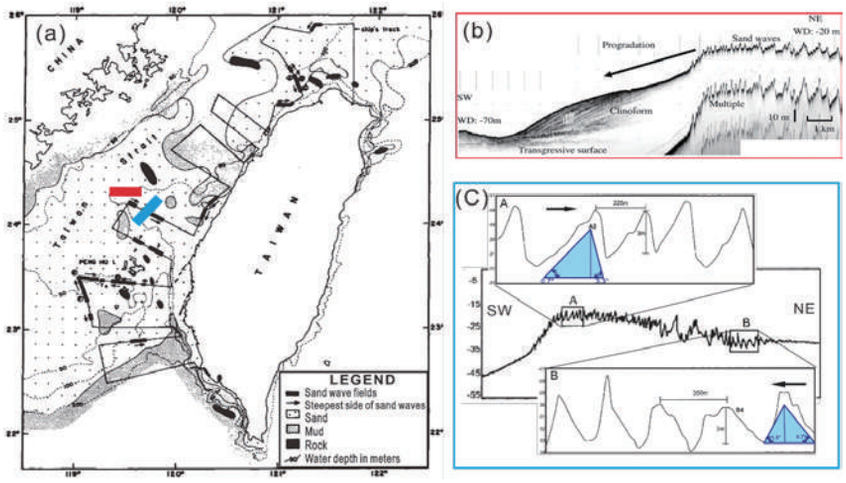

Figure 6. (a) The sand wave distribution and sediment types in the Taiwan Strait (modified from Boggs, 1974); (b) chirp sonar profiles show subaqueous delta prograde southwestward off the Choshui River mouth, while the Topset of the clinoform is dominated by distinct sand waves, 2–5 m high (modified from Liu et al., 2008), and (c) there are two different shapes of sand waves distinguished from the bathymetric profile. (modified from Liao and Yu, 2005)

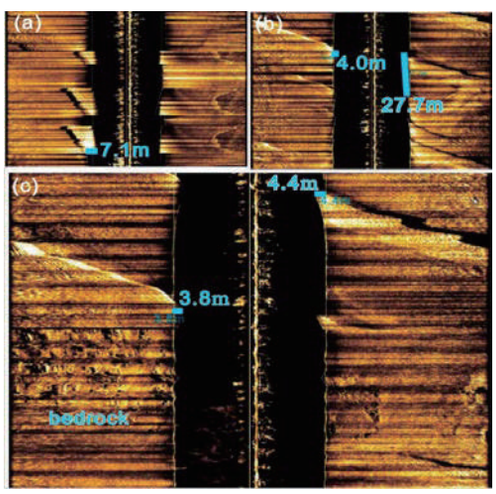

Figure 7. Three different shapes of sand wave are defined from side-scan sonar images: (a) unimodal-shaped sand waves, (b) curve-shaped sand waves, and (c) the outcropping bedrock accompanied with sand waves. (modified from Hu et al., 2013)

Marine Research of the National Academy of Marine Research
DOI: 10.29677/MR.202112_1(1).0001

In the southern Taiwan Strait, the Taiwan Shoal exhibits a lobe-shaped area with a water depth of less than 40 m. The Taiwan Shoal hosts relict sediment remnant from deltaic deposits during the last glacial period. Different estimations of Taiwan Shoal boundaries (Figure 8a) indicate the migrating sand waves, while the sand waves gradually disappeared toward the deeper depth (Figure 8b). Note that the landward sand waves are gentler than the seaward, indicating that the tidal current modifies the sand waves from northeast to the southeast (Figure 8c) (Hu et al., 2013).

Extreme events substantially influence sediment aggregation and movement in the Taiwan Strait. Chang et al. (2010) found that the typhoon-induced surface flows were amplified in the long, narrow geometry of the Taiwan Strait. The Ekman drift could explain the typhoon-induced surface currents. Extreme weather events may trigger terrestrial materials from western Taiwan to offshore northeast Taiwan (He et al., 2014). Zhang et al. (2010) suggests that the strong tidal currents and storm-induced currents along the channel might enhance the tide-surge interaction via nonlinear bottom friction, resulting in strong oscillations along the northern Taiwan Strait. Figure 9 shows the composite satellite-derived transparency images after Typhoon Morakot in 2009, revealing three turbid waters from different sources triggered by Typhoon Morakot were even transported to the region offshore of NE Taiwan.

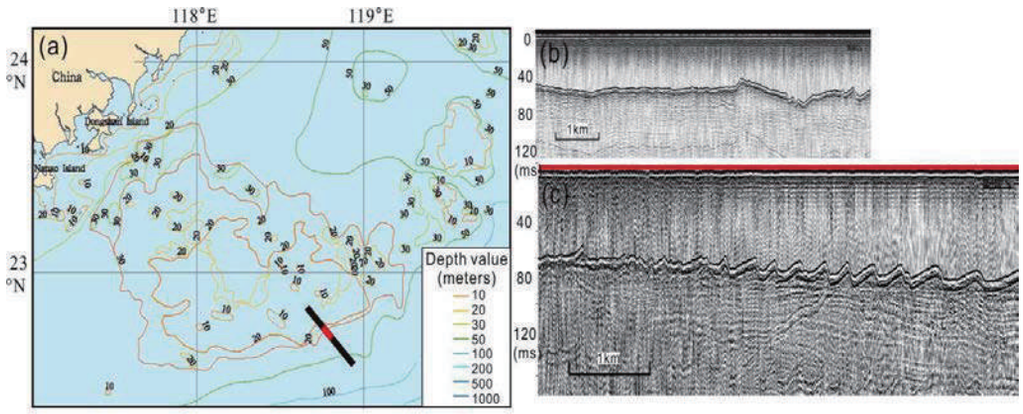

Figure 8. (a) The estimated boundaries of Taiwan Shoal and (b) the sand waves gradually disappeared at depth in southeast profile. (c) The landward sand waves are gentler than those seaward, indicating that the tidal current shapes the sand waves from northwest to the southeast. (Hu et al., 2013)

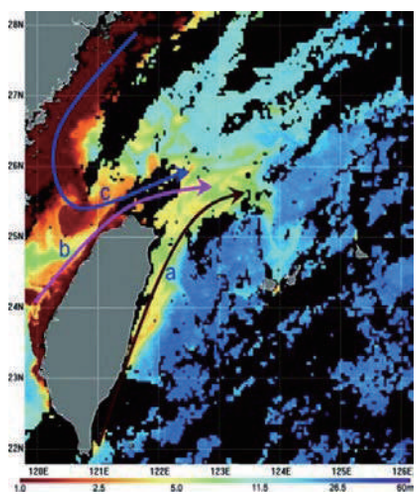

Figure 9. The composite satellite-derived transparency images after Typhoon Morakot (2009). The three arrows show the three turbid waters triggered by Morakot. These waters were transported to the region offshore of northeastern Taiwan. (Zhang et al., 2010)

DOI: 10.29677/MR.202112_1(1).0001

3 METHODOLOGY

Understanding the sand wave dynamics provides critical information to offshore engineering and marine ecology. The migration of sand waves is dominated by the interaction processes between the seabed sediments and bottom currents, and is related to various environmental conditions (Boggs, 1974; Blatt et al., 1980; Ashley, 1990). Therefore, to understand the factors between these two phases, it is crucial to define the morphology of sand waves by analyzing the topography images using quantitative and qualitative methods. In this study, we analyzed multibeam bathymetric data referring to the latest surveys in the Taiwan Strait.

3.1 Literature Reviews

There are two basic approaches for investigating sand wave dynamics: seabed observations and modeling. Models that provide general knowledge of sand waves to carry out the potential effects of various hydrodynamic components, while the observations record the time-slices of the seabed image. For short-term seabed observations, the movement of the crest of a sand wave was studied using cross-sectional profiles obtained from lines of seabed reference stakes; the results show that the sand wave is relatively stable at neap tides, while at higher tidal ranges, the crest position oscillated with successive flood and ebb tides (Figure 10a & 10b) (Langhorne, 1982). For yearly seabed observations conducted in 2011, 2012, and 2013, the results suggest that the giant sand waves act as a bathymetric obstacle, thus changing the direction of bottom currents flowing over them and resulting in a change in sediment transport pattern on the Taiwan Shoal (Figure 10c) (Zhou et al., 2018a). On the other hand, for the seabed modeling strategy, considering the sand wave migration through modeling the typhoon effect, the speed variation of the bottom currents increased from 22 to 44 cm/s according to the ROMS simulation of the flow velocity in northern SCS during Typhoon Fanapi in 2010 (Zhou et al., 2018b). Furthermore, the sand wave migration calculated using Rubin's formula with bottom currents suggests that the sand waves might have migrated 2-2.9 meters during Typhoon Fanapi, which accounts for 10 to 26% of the annual migration distance, as the annual sand wave migration rate is about 5.8-19 m (Figure 11). Nevertheless, it may not be reasonable to extrapolate the migration rate of the sand waves over long periods without detailed geometric studies.

The Taiwan Strait hosts two significant convex terrains, the Changyun Ridge to the east and the Taiwan Shoal to the south. The western Changyun Ridge is a tide-dominated linear NW-SE trending sand ridge perpendicular to the western coast of Taiwan (Figure 12a). The large to huge sand waves mainly occur in the western Changyun Ridge, implying that the western Changyun Ridge is presently active compared to the currently inactive or moribund eastern Changyun Ridge (Liao and Yu, 2005). Giant sand waves also spread in the Taiwan Shoal (Figure 12b) (e.g., Hu et al., 2013; Bao et al., 2014; Yu et al., 2015; Zhou et al., 2018a). Yu et al. (2015) discuss the characteristics and distribution of the giant sand waves, while Bao et al. (2014) classify the cation of the small sand waves according to waveforms and propagation patterns of the small sand waves existing between giant sand wave peaks (Figure 13). Two remarkable features of sand waves were identified in the Taiwan Shoal (Zhou et al., 2018a). One is the divergent pattern of giant sand waves regarding the propagation trends, and the other is the crest-parallel migration feature of small sand waves, which differs from the classical crest-perpendicular migration.

Although different research approaches may lead to different speculations, the initial static analysis should focus on the seabed geometry as the initial status. Therefore, we analyzed the topographic images to better understand the sand wave geometry as a preliminary study on sand waves in the study area. The multibeam bathymetric data reveal coexisting sand waves with distinct spatial scales in the Changyun Ridge and Taiwan Shoal.

DOI: 10.29677/MR.202112_1(1).0001

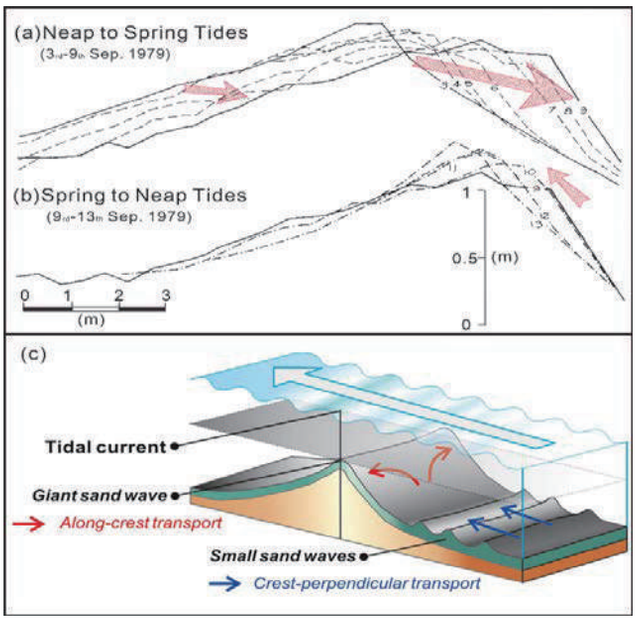

Figure 10. The directions (arrows) read from the crest profiles (a and b), measured at the end of ebb tides in September 1979, indicate the progressive bedform movement (after Langhorne, 1982). (c) The diagram shows that the shift of bottom currents influences the sediment transport patterns as they impact the giant sand waves. The grey arrows denote the primary orientation of the giant sand waves, while blue arrows show the primary migration vector directions, and the red arrows indicate orientations of the major axis of the dominant tidal ellipse. Note that the crest-perpendicular sand wave migration (blue arrows) only occurs by normal bottom current flow across small sand waves distal to the giant sand waves. (after Zhou et al., 2018a)

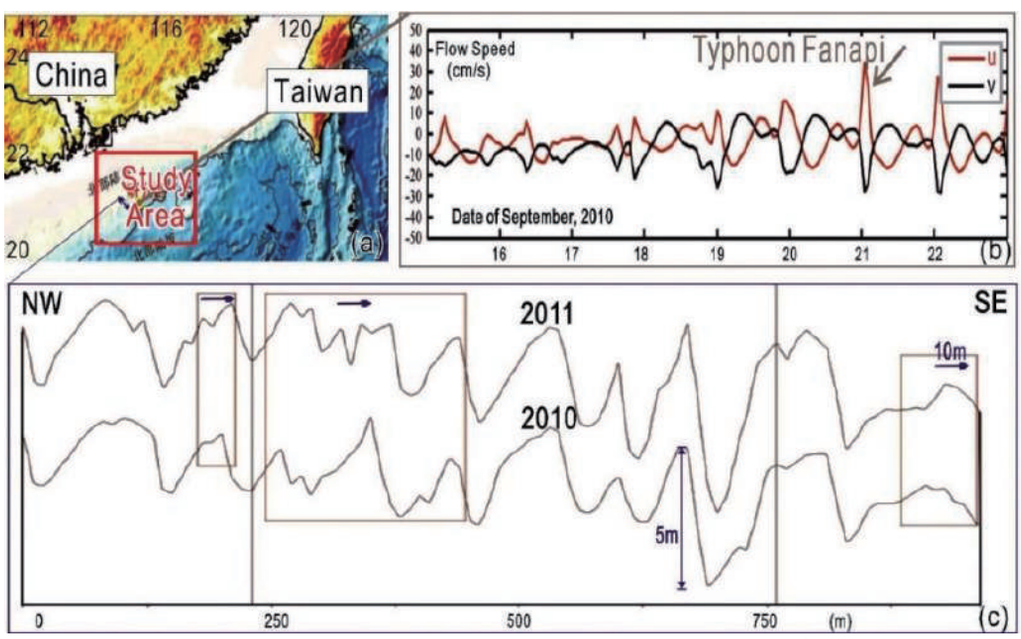

Figure 11. (a) In northern SCS, (b) the time series of bottom flow speed during Typhoon Fanapi shows a distinguished variation of velocities in E-W (u) and N-S (v) directions, and (c) the profile comparison demonstrates the huge sand waves migration before and after Typhoon Fanapi. (after Zhou et al., 2018b)

DOI: 10.29677/MR.202112_1(1).0001

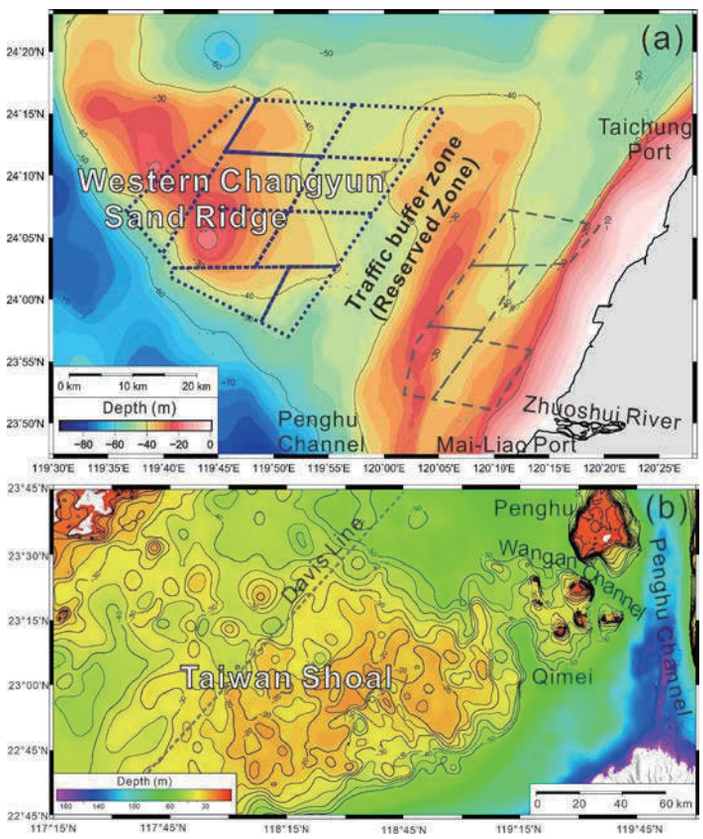

Figure 12. Topographic maps of the Changyun Sand Ridge and Taiwan Shoal illustrate the regional geological features. (Bathymetric data source: Ocean Data Bank)

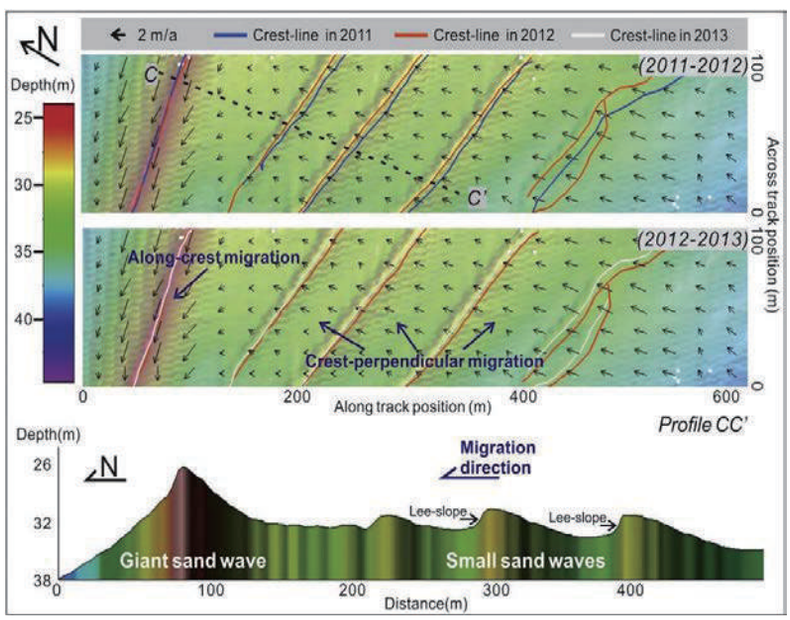

Figure 13. Sand wave migrations in the northwestern Taiwan Shoal during 2011–2012 (top) and 2012–2013 (middle). Both the migration vectors and the shift of the crest-lines of the small sand waves in 2011 (blue), 2012 (orange), and 2013 (gray) indicate northward migration direction, which also coincides with the steeper northern slopes of the small sand wave profiles (Profile CC'). (Zhou et al., 2018a)

Marine Research of the National Academy of Marine Research
DOI: 10.29677/MR.202112_1(1).0001

3.2 Geomorphodynamic Analysis

Allen (1980) summarized the experimental results and pointed out that the water flow and sand wave has the evolutionary order of linear, chain, tongue, crescent, and diamond along with the increase of flow velocity, which becomes the basis of sand wave shape classification. There are many general quantitative and qualitative description methods used to analyze the geometric characteristics of sand waves, including describing its size and shape quantified by the cross-section with peak and valley information and the spatial characteristics described by 3D topographic data (Figure 14). The prototypes of the bedform concerning wave height/wavelength ratio may divide the submarine sand waves into two different main classes: symmetrical/trochoidal and asymmetrical/progressive waves (e.g., Van Veen, 1935; Sterlini et al., 2009). The asymmetry (***A***) of sand waves is defined by subtracting the distance from the crest to the trough of a gentle slope (stoss side) or steep slope (lee side) ($\boldsymbol{L_1}$ and $\boldsymbol{L_2}$, respectively), divided by the total length of the sand wave (***L***) (Knaapen, 2005) (Figure 14a). Moreover, the trochoidal sand waves are generated within a circle advancing constant velocity ***V*** rolls along the flow direction. In contrast, the circumference of the circle is equal to one wavelength (***L***), and wave height (***H***) equals twice the distance from the center of the circle, where r = radius of the circle, and the generating point will pass over the wave as a particle traveling under the influence of gravity with average velocity ***V*** (Tricker, 1964) (Figure 14b). The basic definition of these prototypes of the bedform guides us to classify the sand wave geometry. However, other characteristic bedforms may also be distinguished other than the two referred classes.

Multibeam bathymetric data provides specific bedform information from different prospecting views since the shape of sand waves reflects the appearance and dynamic environment of the bedform, while the shape's evolution is based on the changes of the wave crests. Regarding the geomorphologic analysis of sand waves, the 2D and 3D topographic plots can indicate the development of underwater sand waves on the seabed (Song, 2019). Two types of sand waves are distinguished, NNW-SSE orientation long bed waves and E-W alignment small-magnitude sand waves, based on analyzing the crests from 2D plane view (Figure 15a); studying the sand wave characteristics along the cross-section profiles derived from the 3D topography allows us to interpret the geometric variations clearly (Figure 15b). Furthermore, comparing the seabed images acquired from repeating surveys could provide the azimuth and velocity information of the sand waves migration (Figure 15c).

This study focuses on classifying the sand wave morphological characteristics in the western Changyun Ridge and Taiwan Shoal, where the water depth ranges from 15 to 65 m in the Taiwan Strait (Figure 16). The length and width of the western Changyun Ridge are 53 km and 26 km, respectively, and has a long axis trending in an NW-SE direction. The length and width of the Taiwan Shoal are 180 km and 80 km, respectively, and has a long axis trending in an E-W direction. The average water depth in the Taiwan Shoal is about 20 m, and the center part is the shallowest area, where it gradually deepens in all directions. To understand the distribution, characteristics, forming mechanism, and migration behaviors of the sand waves within these two regions, we collected and analyzed previous topography profiles derived from the multibeam bathymetric data (Yu et al., 2015; Zhou et al., 2018a; Preparatory Office of Greater Changhua Offshore Wind Farm Ltd., 2018; Preparatory Office of Haiding International Investment Co., Ltd. 2018; Preparatory Office of Hai Long Wind Power Co., Ltd. 2018). The geometry and movement of the sand waves were studied using cross-sectional profiles and the crest-lines distribution obtained from the topographic reference, combined with previous geophysical, geological, ocean current, and tidal data in the study area, may provide us the background information to speculate on the possible constant process occurred in the corresponding bedform.

DOI: 10.29677/MR.202112_1(1).0001

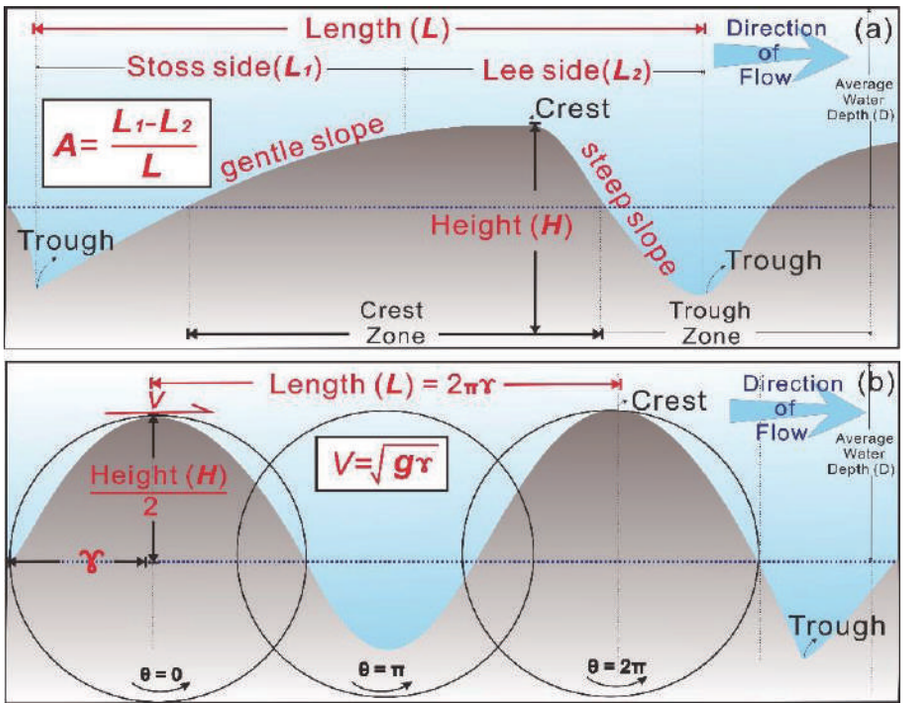

Figure 14. The cross-section illustrates the schematic of asymmetrical and trochoidal sand waves, with the equation for calculating the level of asymmetry (A), a dimensionless value to describe wave height (H)/ wavelength(L) ratio. (after Allen, 1980 and Hand, 1969)

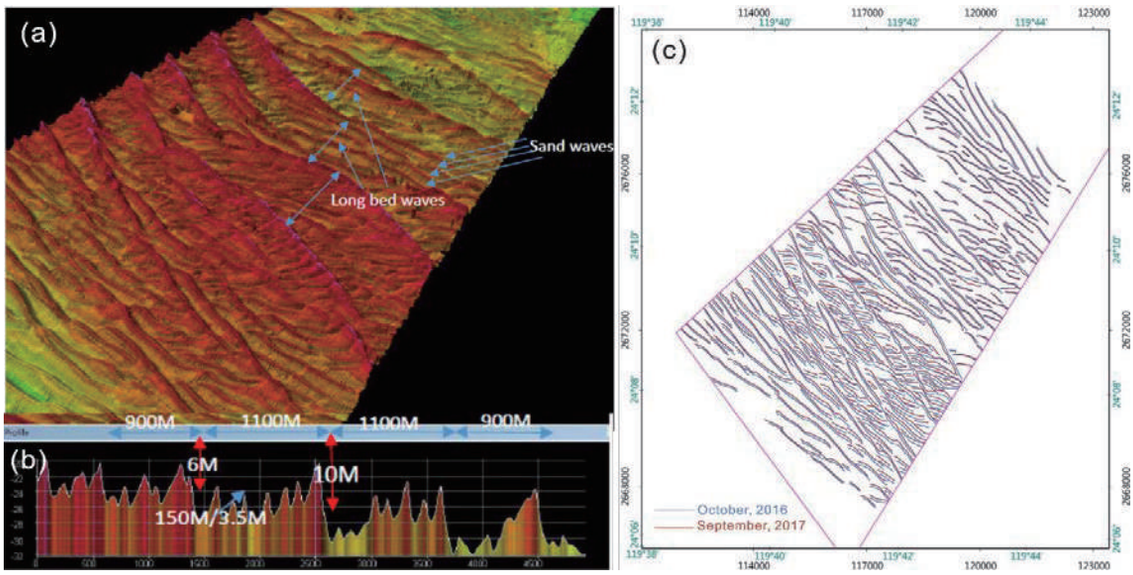

Figure 15. The (a) 2D and (b) 3D topography plots are capable of indicating the sand wave development on the seabed, (c) the repeating bathymetry surveys may quantify the sand wave migration. (after Song, 2019)

Marine Research of the National Academy of Marine Research
DOI: 10.29677/MR.202112_1(1).0001

4 SAND WAVE CHARACTERIZATION FROM BATHYMETRIC DATASETS

Multibeam bathymetric data recently collected by the offshore wind farm projects in the western Changyun Ridge (Preparatory Office of Greater Changhua Offshore Wind Farm Ltd., 2018; Preparatory Office of Haiding International Investment Co., Ltd. 2018; Preparatory Office of Hai Long Wind Power Co., Ltd. 2018) infer that the densely distributed sand waves (especially at zone 11. 14, and 16 to 19) can be classified into several distinct bedform patterns (Figure 16). On the other hand, the spatial distribution of giant sand waves in the Taiwan Shoal were imaged by the remoting sensing technique, and it can be compared with multibeam bathymetric data for deriving the geometric information of sand waves (Figure 17). They provide us the bedform information to study the sand wave distribution and geometry, as follows.

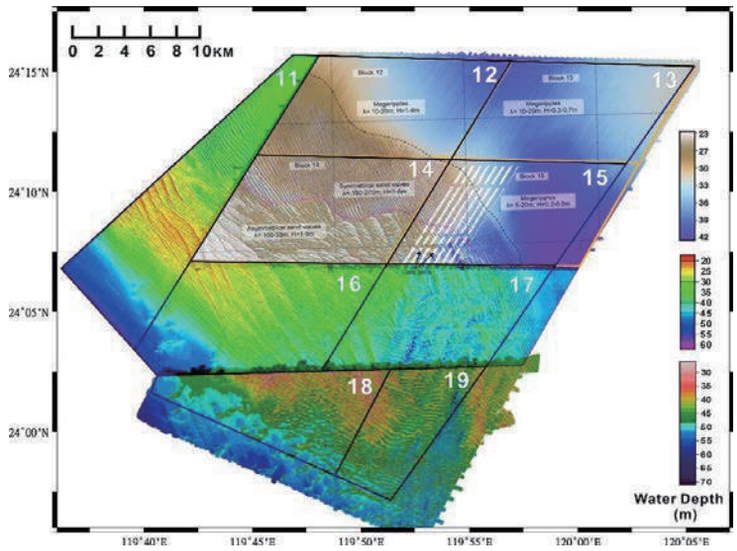

Figure 16. Integrated topographic maps in the western Changyun Ridge extracted from the environmental impact statement (EIS) reports. (after Preparatory Office of Greater Changhua Offshore Wind Farm Ltd., 2018; Preparatory Office of Haiding International Investment Co., Ltd. 2018; Preparatory Office of Hai Long Wind Power Co., Ltd. 2018)

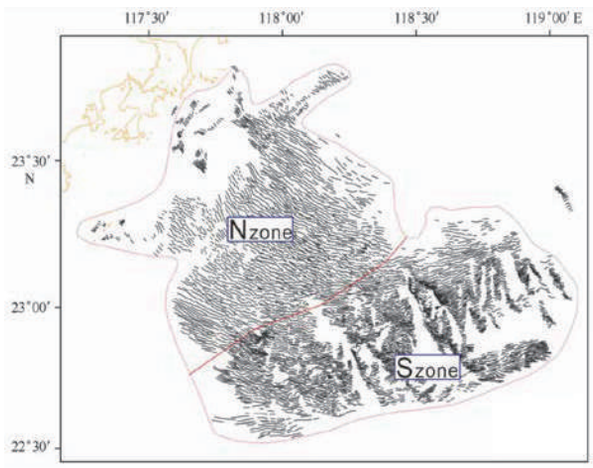

Figure 17. Map showing the sand wave crests (black line) in the Taiwan Shaol. The red line represents the Orientation Changing Limit that separates the NW-SE trending sand wave field (Nzone) from the NE-SW trending sand wave field (Szone) (Zhou et al., 2018b) that were extracted from satellite images. (Yu et al., 2015)

DOI: 10.29677/MR.202112_1(1).0001

4.1 Sand Wave Crest-lines

The sand wave crest-lines in the whole Taiwan Shoal were extracted from two high-quality HJ-1A/B satellite images by the sun glitter inversion method (Zhang et al., 2014), the sand waves mainly oriented in NW-SE (orange lines) and W-E (green lines) directions, coinciding with the giant sand wave crest-lines derived from multibeam bathymetry data (Yu et al., 2015). The synthetic-aperture radar (SAR) images show that the crest lengths and wavelengths of the sand waves range from 500–5,000 m and 200–2,000 m, respectively. Zhou et al. (2018b) defined a so-called Orientation Changing Limit (OCL) based on the giant sand wave propagation pattern: On the northern side of OCL, the average direction of giant sand waves is 132°, and it becomes W-E with an average direction of 83° on the southern side; accordingly, the sand waves in the north area present a north or northeast migrating trend while the sand waves in the south area migrate southward, based on the analysis of waveforms (Figure 17).

The integrated topography maps (Figure 16) extracted from the environmental impact statement (EIT) reports (Preparatory Office of Greater Changhua Offshore Wind Farm Ltd., 2018; Preparatory Office of Haiding International Investment Co., Ltd. 2018; Preparatory Office of Hai Long Wind Power Co., Ltd. 2018) allow us to distinguish the orientations of the sand wave crest-lines in the western Changyun Ridge (Figure 18). The sand waves in the north to the central portion of the area are mainly oriented in NW-SE (red lines) with an average azimuth of 344°. In contrast, the sand waves in the south strike in E-W (green lines) with an average direction of 155°. In addition, the thicker NW-SE striking purple lines in Figure 18 have an average azimuth of 344°, indicating the different migration trends between the giant sand waves and the smaller ones.

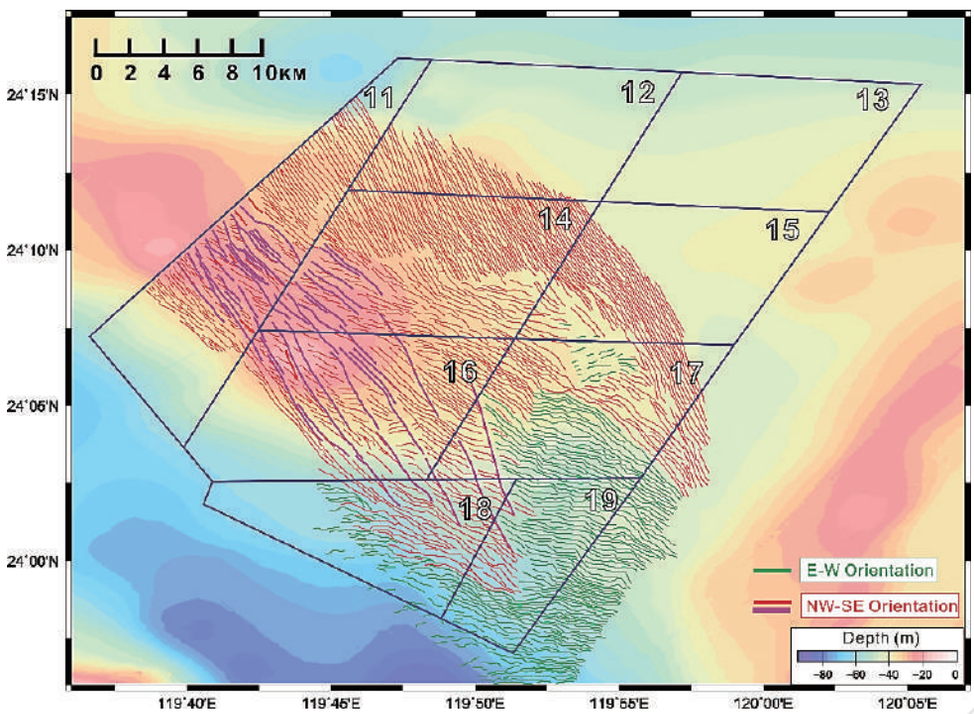

Figure 18. Bathymetric map overlaid by the sand wave crest-lines distinguished from Figure 15, illustrating that the sand wave crests in the Changbin offshore wind farm mainly strike in the NW-SE (red and purple lines) and W-E (green lines) directions.

DOI: 10.29677/MR.202112_1(1).0001

4.2 Sand Wave Geometries

Two parameters quantitatively describe the size of the sand wave: wavelength and height (amplitude). Wavelength is the horizontal distance between two adjacent wave troughs and can be divided into the length of the two wings of the sand wave by the horizontal distance between the two wave crests and the wave crest. The wave height is the vertical distance from the crest to the line connecting the two wave troughs. Here we identify the shapes and dimensions of the sand waves by analyzing the cross-sections derived from the topographic profiles.

The results show that the average height of the sand waves in the Taiwan Shoal is about 13.5 m, which is about two-thirds of the background water depth, and the wavelengths of the sand waves are mostly 500–700 m. The sand wave heights in the Taiwan Shoal range from 4.5 to 22.5 m, while the wavelengths range from 244 to 2,115 m, revealing coexisting sand waves with two distinct spatial scales. One is the divergent pattern of giant sand waves regarding the propagation trends, giant sand waves with a length of ~750 m and height of ~15 m, and small sand waves with lengths of 30-100 m and height of ~1.5 m (Zhou et al., 2018a). Through analyzing seven tracks of the multibeam bathymetric dataset, Yu et al. (2015) recognized three types of sand waves from the characteristics of their bedform shapes (Figure 19). The trochoidal sand waves cover almost the entire area, while the sinusoidal and bimodal sand waves are observed in the middle and western parts of the shoal, respectively. Furthermore, based on studies of the symmetry index and geometries of 434 giant sand waves from the bathymetric swath, the spatial distribution of giant sand waves in the Taiwan Shoal could be divided into four types on topographic profiles (Figure 20): double-crested (Dc-type), symmetrical (S-type), asymmetrical (A-type), and symmetrical-asymmetrical (S-A-type) sand waves (Zhou et al., 2020). A Dc-type sand wave unit comprises two sand wave crests of similar height, with the largest wavelength ranging from 866 to 2,115 m. The S-type and S-A-type sand waves are ubiquitous in tidal environments and usually coexist on the central and eastern parts of the Taiwan Shoal, respectively (Table 1).

In the western Changyun Ridge, the average height of the sand waves is about 6 meters, and the dominant wavelengths fall between 200–250 m, while the heights and wavelengths range between 0.3 to 10 m and 5 to 1,700 m, respectively (Preparatory Office of Greater Changhua Offshore Wind Farm Ltd., 2018; Preparatory Office of Haiding International Investment Co., Ltd. 2018; Preparatory Office of Hai Long Wind Power Co., Ltd. 2018). We identified five types of coexisting sand waves by analyzing over 500 sand wave geometries recognized from the topographic profiles in the western Changyun Ridge (Figure 22~22). The sizes and shapes of the bedform compiled from these cross-sections are classified into (a) long bed trochoidal (LT-type), (b) symmetrical (S-type), (c) trochoidal (T-type), (d) sinusoidal (Sin-type) sand waves, and (e) mega-ripples (Mr-type) (Preparatory Office of Greater Changhua Offshore Wind Farm Ltd., 2018; Preparatory Office of Haiding International Investment Co., Ltd. 2018; Preparatory Office of Hai Long Wind Power Co., Ltd. 2018). The Lt-type sand waves possess the largest dimension in the western Changyun Ridge, where the slope of the NE flank is steeper than the SE, and there are many small-scale sand waves between the wave ridges (Figure 21a). The S-type sand waves occur in the NE portion of the western Changyun Ridge (Figure 21b) with symmetrical shape for the flanks at both sides. The T-type sand waves distribute over the center of the western Changyun Ridge (Figure 21c) with the NW-SE and E-W crest-line trending in the western and eastern portions, respectively (Figure 21d). The Sin-type sand waves spread over the southern portion of the western Changyun Ridge (Figure 21e).

DOI: 10.29677/MR.202112_1(1).0001

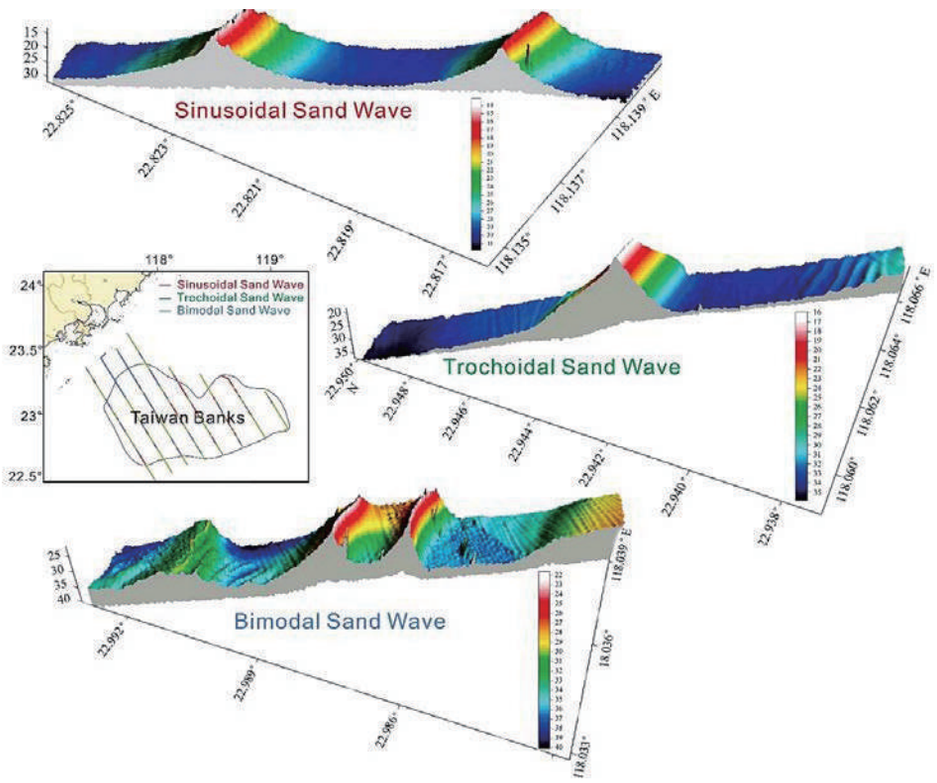

Figure 19. Distribution of the three kinds of sand waves in the Taiwan Shoal. (After Yu et al., 2015)

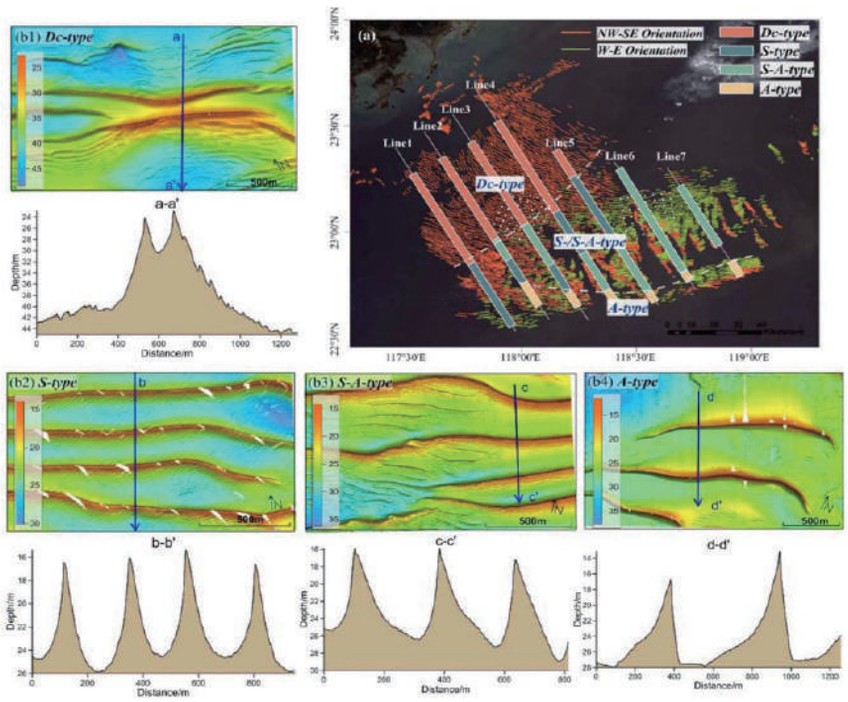

Figure 20. Map showing the four types of giant sand waves identified on topographic profiles in the Taiwan Shoal (a) (Zhou et al., 2020), including (b1) double-crested (Dc-type), (b2) symmetrical (S-type), (b3) symmetrical-asymmetrical (S-A-type), and (b4) asymmetrical (A-type) sand waves.

DOI: 10.29677/MR.202112_1(1).0001

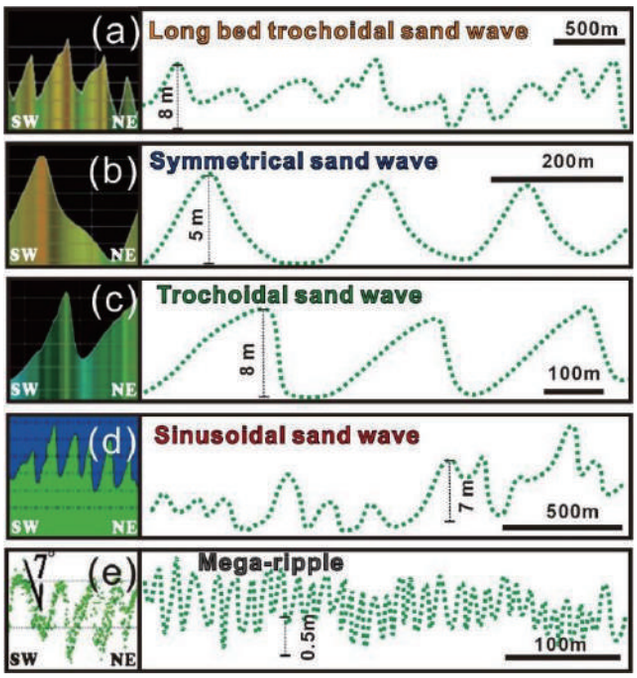

Figure 21. Five types of sand wave geometries were identified on topography profiles in the western Changyun Ridge. The locations of the cross-sections are mapped in Figure 20. (Redrawn after Preparatory Office of Greater Changhua Offshore Wind Farm Ltd., 2018; Preparatory Office of Haiding International Investment Co., Ltd. 2018; Preparatory Office of Hai Long Wind Power Co., Ltd. 2018)

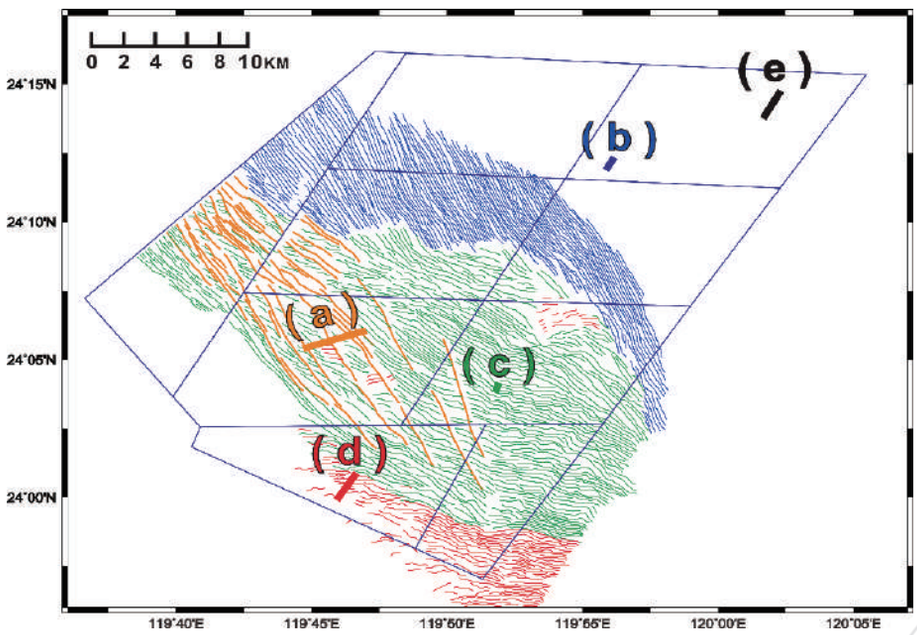

Figure 22. The distribution of the five types of sand waves in the western Changyun Ridge, (a) long bed trochoidal (Lt-type) (orange lines), (b) sinusoidal (Sin-type) (blue lines), (c) trochoidal (T-type) (green lines), (d) symmetrical (S-type) (red lines) sand waves, and (e) mega-ripples (Mr-type).

DOI: 10.29677/MR.202112_1(1).0001

Table 1. Sand wave geometries and bedform environments in the Taiwan Shoal. (compiled from Zhou et al., 2018a; Zhou et al., 2020)

Type	Double-crested sand wave	Symmetrical sand wave	Symmetrical-Asymmetrical sand wave	Asymmetrical sand wave
Orientation of crest-lines	NW-SE	NW-SE	W-E	W-E
Accounting (%)	21	41	30	8
Wave length (m)	866-2,115	247-1,285	250-1,200	244-585
Wave height (m)	7-17	22.5-37	5-22	4.5-10
Water depth (m)	30-46	32-36	26-30	32-48
Grain size (mm)	0.35-0.75	0.4-0.7	0.4-.65	0.4-0.6
Migration trend	WNW	SE	SSE	S
Migration rate (m/y)	1~5	1~4	1~3	1~2

5 DISCUSSION

Sand waves consequently grow from sediment transportation and converge from troughs to crests. Local hydrodynamic conditions often give rise to various grain-sorting phenomena, leading to either symmetrical or asymmetrical shapes (Lefebvre et al., 2016). The sea-level fluctuations and sustained sediment flux from the western rivers of Taiwan also influence the sand wave geomorphologic distribution. Furthermore, extreme events with huge turbulent depositions could reproduce the bedform environments. Maximum wave heights of 4.7m (winter) and 6.5m (summer) have been recorded. Several typhoons pass through the Taiwan Shoal every year, causing significant damage to the seabed patterns (Bao et al., 2014). However, the storm waves in the northern South China Sea (water depth ~130 m) are unlikely to significantly influence the seabed, although typhoon events are frequent (Wang and Li, 1994; Schijen, 2017). As a result, we need to define an initial bedform status based on bathymetric datasets before deducing the potential sediment migrations by time-lapse images. Note that we cannot extrapolate sand wave migrations over long periods as wind stress and surface wave activity interrupt the dynamic tidal trends.

The identified characteristics of sand wave geometries in the western Changyun Ridge and Taiwan Shoal display few similarities insinuating that they may be affected by different morphodynamical factors, though they are situated with coincidental water depth and location in the Taiwan Strait. The variable orientation of the steepest faces of the sand waves indicates that the pattern of the bottom current movements here is very complex. The S-type or S-A type sand waves occupied over 70% of the Taiwan Shoal area, while the T-type and LT-type were distributed about 60% of the western Changyun Ridge (Table 1 & 2). The symmetrical sand waves in the two areas have a distinct difference in size. The wavelengths and heights of the S-type sand waves in the Taiwan Shoal are five times greater than those in the western Changyun Ridge, while the grain size might be the key

DOI: 10.29677/MR.202112_1(1).0001

factor allowing the bedform to develop different levels of the sand waves (Ernstsen et al., 2005). The wave heights in the Taiwan Shoal are higher than those in the western Changyun Ridge might insinuate that the sculpting effect, from bottom current to seabed sediments, are vigorously reduced since the migration rates also imply corresponding consequences. It appears that the largest wave heights correlate to lower geohazard impacts since they generally have lower migration rates in the Taiwan Strait. On the contrary, long-term monitoring of the widely distributed sand waves with high migration rates is recommended to ensure offshore engineering safety.

Table 2. Sand wave geometries and bedform environments in the western Changyun Ridge. (Compiled from Preparatory Office of Greater Changhua Offshore Wind Farm Ltd., 2018; Preparatory Office of Haiding International Investment Co., Ltd. 2018; Preparatory Office of Hai Long Wind Power Co., Ltd. 2018)

Type	Long bed trochoidal sand wave	Symmetrical sand wave	Trochoidal sand wave	Sinusoidal sand wave	Mega-ripples
Orientation of crest-lines	NW-SE	NW- SE	NW-SE and WNW-ESE	W-E	WNW-ESE
Accounting (%)	7	21	52	17	3
Wave length (m)	1,000~1,700	150~250	200~300	150~250	5~25
Wave height (m)	6~10	4~6	6~10	4~6	0.3~4
Water depth (m)	30-46	22-42	22-40	32-48	32-42
Grain size (mm)	0.08-0.34	0.13-0.14	0.16-0.28	0.25-0.38	0.14-0.16
Migration trend	NE	NE	N and NE	N and NE	NE
Migration rate (m/y)	1~5	1~5	tens	tens	tens

6 CONCLUSIONS

We classified the sand waves of the Changyun Sand Ridge and Taiwan Shoal through compiling and analyzing the crest-line distribution and geometries of the sand waves as a preliminary study in the Taiwan Strait. Our results indicate that the characteristics of sand waves in the Taiwan Shoal and western Changyun Ridge are quite variable. Five types of sediment waves with different morphologic characteristics, migration directions, and possible migration rates are documented. It seems that the bottom currents constantly shape the seabed and drive the sand wave migration, while the density flows (e.g., debris flow or turbidite) occasionally change the seabed topography. Nevertheless, it is difficult to understand the seabed erosion/deposition processes without time-dependent bathymetric data. Since sand wave migration can lead to substantial topographic change and contribute to seabed instability, further time-dependent bathymetric and oceanographic observations are required.

DOI: 10.29677/MR.202112_1(1).0001

ACKNOWLEDGEMENTS

We acknowledge the Ocean Data Bank, Taiwan, for the compiled bathymetric data. We are grateful to the offshore wind developers and the Environmental Protection Administration, Taiwan, for releasing the public Environmental Impact Statement (EIS) reports.

REFERENCES

Allen, J. R. L. (1980). Sand Waves: A Model of Origin and Internal Structure. *Sedimentary Geology, 26*(4), 281-328. https://doi.org/10.1016/0037-0738(80)90022-6

Amos, G. L., & King, E. L. (1984). Bedforms of the Canadian Eastern seaboard: a comparison with global occurrences. *Marine Geology, 57*(1-4), 167-208. https://doi.org/10.1016/0025-3227(84)90199-3

Ashley, G. M. (1990). Classification of Large-Scale Subaqueous Bedforms: A New Look at an Old Problem. *Journal of Sedimentary Research, 60*(1), 160-172. https://doi.org/10.2110/jsr.60.160

Bao, J., Cai, F., Ren, J., Zheng, Y., Wu, C., Lu, H., & Xu, Y. (2014). Morphological Characteristics of Sand Waves in the Middle Taiwan Shoal Based on Multi-beam Data Analysis. *Acta Geologica Sinica-English Edition, 88*(5), 1499-1512. https://doi.org/10.1111/1755-6724.12314

Barnard, P. L., Erikson, L. H., & Kvitek, R. G. (2011). Small-scale sediment transport patterns and bedform morphodynamics: New insights from high-resolution multibeam bathymetry. *Geo-Marine Letters, 31*(4), 227–236. https://doi.org/10.1007/s00367-011-0227-1

Besio, G., Blondeaux, P., Brocchini, M., & Vittori, G. (2004). On the modeling of sand wave migration. *Journal of Geophysical Research: Oceans, 109*(C4). https://doi.org/10.1029/2002JC001622

Blatt, H., Middleton, G. V., & Murray, R. C. (1980). *Origin of Sedimentary Rocks.* Englewood Cliffs, New Jersey, Prentice-Hall, Inc.

Boggs, S.,-Jr. (1974). Sand Wave Fields in Taiwan Strait. *Geology 2*(5), 251-253. https://doi.org/10.1130/0091-7613(1974)2<251:SFITS>2.0.CO;2

Cai, A., Zhu, X., Li, Y., et al. (1992). Sedimentary environment in Taiwan Shoal. *Chinese Journal of Oceanology and Limnology, 10*(4), 331–339. https://doi.org/10.1080/0264041031000071029

Chang, Y. C., Tseng, R. S., & Liu, C. T. (2008). Evaluation of Tidal Removal Method Using Phase Average Technique from ADCP Surveys along the Peng-Hu Channel in the Taiwan Strait. *Terrestrial, Atmospheric and Oceanic Sciences, 19*(4), 433-443. https://doi.org/10.3319/TAO.2008.19.4.433(Oc)

Chang, Y. C., Tseng, R. S., & Centurioni, L. R. (2010). Typhoon-induced strong surface flows in the Taiwan Strait and Pacific. *Journal of Oceanography, 66*(2), 175-182. https://doi.org/10.1007/s10872-010-0015-y

Dorst, L. L., Roos, P. C., & Hulscher, S. J. M. H. (2011). Spatial differences in sand wave dynamics between the Amsterdam and the Rotterdam region in the Southern North Sea. *Continental Shelf Research, 31*(10), 1096-1105. https://doi.org/10.1016/j.csr.2011.03.015

Dyer, K. R., & Soulsby, R. L. (1988). Sand transport on the continental shelf. *Annual Review of Fluid Mechanics, 20*, 295–324. https://doi.org/10.1146/annurev.fl.20.010188.001455

Ernstsen, V. B., Noormets, R., Winter, C., Hebbeln, D., Bartholomä, A., Flemming, B. W., & Bartholdy, J. (2005). Development of subaqueous barchanoid-shaped dunes due to lateral grain size variability in a tidal inlet channel of the Danish Wadden Sea. *Journal of Geophysical Research: Earth Surface, 110*(F4). http://doi.org/10.1029/2004JF000180

Games, K. P., & Gordon, D. I. (2015). Study of sand wave migration over five years as observed in two windfarm development areas, and the implications for building on moving substrates in the North Sea. *Earth and Environmental Science Transactions of the Royal Society of Edinburgh, 105*(4), 241-249. https://doi.org/10.1017/S1755691015000110

Guan, M. (2017). *Sand wave numerical simulation in Taiwan Strait*[Unpublished master thesis]. Dalian University of Techonology, pp. 80.

Hand, B. M. (1969). Antidunes as trochoidal waves. *Journal of Sedimentary Research, 39*(4), 1302-1309. https://doi.org/10.1306/74D71E15-2B21-11D7-8648000102C1865D

He, X., Bai, Y., Chen, C. T. A., Hsin, Y. C., Wu, C. R., Zhai, W., Liu, Z., & Gong, F. (2014). Satellite views of the episodic terrestrial material transport to the southern Okinawa Trough driven by typhoon. *Journal of Geophysical Research: Oceans, 119*(7), 4490-4504. https://doi.org/10.1002/2014JC009872

Huh, C. A., Chen, W., Hsu, F. H., Su, C. C., Chiu, J. K., Lin, S., Liu, C. S., & Huang, B. J. (2011). Modern (<100 years) sedimentation in the Taiwan Strait: Rates and source-to-sink pathways elucidated from radionuclides and particle size distribution. *Continental Shelf Research, 31*(1), 47-63. https://doi.org/10.1016/j.csr.2010.11.002

Hu, Y., Chen, J., Xu, J., Wang, L., Li, H., & Liu, H. (2013). Sand wave deposition in the Taiwan Shoal of China. *Acta Oceanologica Sinica, 32*(8), 26-34. http://doi.org/10.1007/s13131-013-0338-9

Jan, S., Sheu, D. D., & Kuo, H. M. (2006). Water mass and throughflow transport variability in the Taiwan Strait. *Journal of Geophysical Research: Oceans, 111*(C12012). https://doi.org/10.1029/2006JC003656

Jan, S, Chern, C. S., Wang, J., & Chao, S. Y. (2004). The anomalous amplification of M_2 tide in the Taiwan Strait. *Geophysical Research Letters, 31*(L07308). https://doi.org/10.1029/2003GL019373

Kao, S. J., Jan, S., Hsu, S. C., Lee, T. Y., & Dai, M. (2008). Sediment budget in the Taiwan Strait with high fluvial sediment inputs from mountainous rivers: New observations and synthesis. *Terrestrial, Atmospheric and Oceanic Sciences, 19*(5), 525-546. https://doi.org/10.3319/TAO.2008.19.5.525(Oc)

Knaapen, M. A. F. (2005). Sandwave migration predictor based on shape information. *Journal of Geophysical Research: Earth Surface, 110*(F4). https://doi.org/10.1029/2004JF000195

Langhorne, D. N. (1982). A study of the dynamics of a marine sandwave. *Sedimentology, 29*(4), 571-594. https://doi.org/10.1111/j.1365-3091.1982.tb01734.x

Lefebvre, A., Paarlberg, A. J., & Winter, C. (2016). Characterising natural bedform morphology and its influence on flow. *Geo-Marine Letters. 36*(5), 379–393. https://doi.org/10.1007/s00367-016-0455-5

Liang, W. D., Tang, T. Y., Yang, Y. J., Ko, M. T., & Chuang, W. S. (2003). Upper-ocean currents around Taiwan. *Deep Sea Research Part II: Topical Studies in Oceanography, 50*(6-7), 1085-1105. https://doi.org/10.1016/S0967-0645(03)00011-0

DOI: 10.29677/MR.202112_1(1).0001

Liao, H. R., & Yu, H. S. (2005). Morphology, Hydrodynamics and Sediment Characteristics of the Changyun Sand Ridge Offshore Western Taiwan. *Terrestrial, Atmospheric and Oceanic Sciences, 16*(3), 621-640. https://doi.org/10.3319/TAO.2005.16.3.621(T)

Liu, C. S., Liu, S. Y., Lallemand, S. E., Lundberg, N., & Reed, D. L. (1998). Digital Elevation Model Offshore Taiwan and Its Tectonic Implications. *Terrestrial, Atmospheric and Oceanic Sciences, 9*(4), 705-738. https://doi.org/10.3319/TAO.1998.9.4.705(TAICRUST)

Liu, J. P., Liu, C. S., Xu, K. H., Milliman, J. D., Chiu, J. K., Kao, S. J., & Lin, S. W. (2008). Flux and fate of small mountainous rivers derived sediments into the Taiwan Strait. *Marine Geology, 256*(1-4), 65-76. https://doi.org/10.1016/j.margeo.2008.09.007

Németh, A. A., Hulscher, S. J. M. H., & de Vriend, H. J. (2002). Modelling sand wave migration in shallow shelf seas. *Continental Shelf Research, 22*(18-19), 2795-2806. https://doi.org/10.1016/S0278-4343(02)00127-9

Preparatory Office of Greater Changhua Offshore Wind Farm NW Ltd. (2018). Environmental Impact Statement (EIS) for Greater Changhua NW Offshore Wind Power Program (the definitive edition). Taipei, Taiwan.

Preparatory Office of Greater Changhua Offshore Wind Farm SW Ltd. (2018). Environmental Impact Statement (EIS) for Greater Changhua SW Offshore Wind Power Program (the definitive edition). Taipei, Taiwan.

Preparatory Office of Greater Changhua Offshore Wind Farm NE Ltd. (2018). Environmental Impact Statement (EIS) for Greater Changhua NE Offshore Wind Power Program (the definitive edition). Taipei, Taiwan.

Preparatory Office of Greater Changhua Offshore Wind Farm SE Ltd. (2018). Environmental Impact Statement (EIS) for Greater Changhua SE Offshore Wind Power Program (the definitive edition). Taipei, Taiwan.

Preparatory Office of Haiding One International Investment Co., Ltd. (2018). Environmental Impact Statement (EIS) for Haiding One Offshore Wind Power Program (the definitive edition). Taipei, Taiwan.

Preparatory Office of Haiding Two International Investment Co., Ltd. (2018). Environmental Impact Statement (EIS) for Haiding Two Offshore Wind Power Program (the definitive edition). Taipei, Taiwan.

Preparatory Office of Haiding Three International Investment Co., Ltd. (2018). Environmental Impact Statement (EIS) for Haiding Three Offshore Wind Power Program (the definitive edition). Taipei, Taiwan.

Preparatory Office of Hai Long II Wind Power Co., Ltd. (2018). Environmental Impact Statement (EIS) for Hai Long II Offshore Wind Farm Project (the definitive edition). Taipei, Taiwan.

Preparatory Office of Hai Long III Wind Power Co., Ltd. (2018). Environmental Impact Statement (EIS) for Hai Long III Offshore Wind Farm Project (the definitive edition). Taipei, Taiwan.

Rubin, D. M., & McCulloch, D. S. (1980). Single and superimposed bedforms: a synthesis of San Francisco Bay and flume observations. *Sedimentary Geology, 26*(1-3), 207-231. https://doi.org/10.1016/0037-0738(80)90012-3

Schrijen, E. P. W. J. (2017). *Modelling the influence of storm related processes and their frequencies of occurrence on sand wave dynamics in the North Sea* [Unpublished master thesis]. University of Twente, pp. 79.

Sterlini, F., Hulscher, S. J., & Hanes, D. M. (2009). Simulating and understanding sand wave variation: A case study of the Golden Gate sand waves. *Journal of Geophysical Research: Earth Surface, 114*(F2). https://doi.org/10.1029/2008JF000999

Song, G. S. (2019). *Underwater Sand Waves Analysis in Offshore Wind Farm Construction.* Global Aqua Survey. http://www.globalaquasurvey.com/news/news01.html

Tricker, R. A. R. (1964). *Bores, breakers, waves and wakes: an introduction to the study of waves on water.* American Elsevier, New York.

Van Dijk, T. A. G. P., & Kleinhans, M.G. (2005). Processes controlling the dynamics of compound sand waves in the North Sea, Netherlands. *Journal of Geophysical Research, 110*(F4). https://doi.org/10.1029/2004JF000173

Van Veen, J. (1935). Sand waves in the North Sea. *The International Hydrographic Review, 12*(1).

Wang, C. (2004). Features of monsoon, typhoon and sea waves in the Taiwan Strait. *Marine Georesources & Geotechnology, 22*(3), 133-150. https://doi.org/10.1080/10641190490467477

Wang, S. Y., & Li, D. M. (1994). Dynamic analysis on sand waves in continental shelf slope and continental slope of Pearl River Mouth Basin in South China Sea. *Acta Oceanol Sin, 16*(6), 122–132.

Wright, L.D., & Thom, B.G. (1977). Coastal depositional landforms: A morphodynamic approach. *Progress in Physical Geography: Earth and Environment, 1*(3), 412-459. https://doi.org/10.1177%2F030913337700100302

Wu, C. R., & Hsin, Y. C. (2005). Volume Transport Through the Taiwan Strait: A Numerical Study. *Terrestrial, Atmospheric and Oceanic Sciences, 16*(2), 377-391. https://doi.org/10.3319/TAO.2005.16.2.377(Oc)

Yincan et al, Y. (2017). Submarine Sand Waves and Sand Ridges. *Marine Geo-Hazards in China* (Chapter 2, pp. 523-554). https://doi.org/10.1016/B978-0-12-812726-1.00012-7

Yu, W., Wu, Z. Y., Zhou, J. Q., & Zhao, D. N. (2015). Meticulous characteristics, classification and distribution of seabed sand wave on the Taiwan Bank. *Haiyang Xuebao, 37*(10), 11-25. http://doi.org/10.3969/j.issn.0253-4193.2015.10.002

Yu, H., Yu, H., Wang, L., Kuang, L., Wang, H., Ding, Y., Ito, S. I., & Lawen, J. (2017). Tidal propagation and dissipation in the Taiwan Strait. *Continental Shelf Research, 136*, 57-73. https://doi.org/10.1016/j.csr.2016.12.006

Zhang, W. Z., Shi, F., Hong, H. S., Shang, S. P., & Kirby, J. T. (2010). Tide-surge interaction intensified by the Taiwan Strait. *Journal of Geophysical Research: Oceans, 115*(C6). https://doi.org/10.1029/2009JC005762

Zhang, H. G., Lou, X. L., Shi, A. Q., He, X. K., Guan, W. B., & Li, D. L. (2014). Observation of sand waves in the Taiwan Banks using HJ-1A/1B sun glitter imagery. *Journal of Applied Remote Sensing, 8*(1), 083570. https://doi.org/10.1117/1.JRS.8.083570

Zhou, J., Wu, Z., Jin, X., Zhao, D., Cao, Z., & Guan, W. (2018a). Observations and analysis of giant sand wave fields on the Taiwan Banks, northern South China Sea. *Marine Geology, 406*, 132-141. https://doi.org/10.1016/j.margeo.2018.09.015

Zhou, Q., Sun, Y., Hu, G., Song, Y., Liu, S., & Du, X. (2018b). Research on the migration rule and the typhoon impact on the submarine sand waves of the northern South China Sea. *Haiyang Xuebao, 40*(9), 78-89. http://doi.org/10.3969/j.issn.0253-4193.2018.09.007

Zhou, J., Wu, Z., Zhao, D., Guan, W., Zhu, C., & Flemming, B. (2020). Giant sand waves on the Taiwan Banks, southern Taiwan Strait: Distribution, morphometric relationships, and hydrologic influence factors in a tide-dominated environment. *Marine Geology, 427* (106238). https://doi.org/10.1016/j.margeo.2020.106238